



STUDY ON SHEAR STRENGTH OF RC BEAM-COLUMN JOINTS WITH ECCENTRIC BEAMS BY THREE-DIMENSIONAL FEM ANALYSIS

H. Noguchi¹, T. Kashiwasaki² and J. Hong³

ABSTRACT

Three-dimensional FEM analysis was conducted on joint shear failure type plane RC beam-column joints, using the amount of lateral reinforcement and bond characteristics of beam reinforcement in the joint section, in addition to beam-column joint eccentricity, as parameters. The stress component in the strut direction was analyzed quantitatively. The investigation revealed that, within a joint at ultimate strength, there exists a region in which the amount of compressive force transmitted is almost consistent irrespective of parameters; and that bond characteristics mainly have an effect on stress distribution in the strut-depth direction, while the amount of lateral reinforcement and joint eccentricity mainly have an effect on stress distribution in the strut-width direction. Based on these results, an estimation equation for shear strength of beam-column joints, including those with joint eccentricity, was proposed.

Introduction

The authors previously used the 3-dimensional finite element method (FEM) on reinforced concrete (RC) beam-column joints to investigate the effects of joint eccentricity (Hong and Noguchi 2006) and of slabs and transverse beams (Hong and Noguchi 2008), and demonstrated an increase in ultimate strength resulting from transmission of shear stress in transverse beams and uneven transmission of compressive stress in the eccentric side of an eccentric joint. In this research, 3-dimensional FEM analysis during monotonic loading was conducted with regards to joint shear failure type plane RC beam-column joints, including those with beam-column joint eccentricity. In addition to joint eccentricity, bond characteristics at the joint and amount of lateral reinforcement were used as parameters. The analytical results were examined qualitatively and quantitatively, and a shear strength equation is proposed with a view to applying the analytical results to earthquake resistance design.

Analysis Specimens

The analysis was conducted on imaginary specimens, based on an RC plane beam-

¹Professor and Dean, Dept. of Archit. and Urban Sci., Graduate School of Eng., Chiba Univ., Chiba, Japan

²Assistant Professor, Dept. of Archit. and Urban Sci., Graduate School of Eng., Chiba Univ., Chiba, Japan

³Researcher, Structural Eng. Division, Tokyo Techno Center, JIP Techno Science Corporation, Tokyo, Japan

column joint specimen, without slabs or transverse beams, used by (Ishida and Fujii *et al.* 2001), modifying the beam width so that the eccentricity ratio (eccentricity / column width) is 0.3 or less. The specimens were designed so that they are of a joint shear failure type, whose ultimate strength is reached by crushing of the joint core concrete without incidence of bond deterioration or crushing of beam-end concrete. The eccentricity was varied between 0 and 25 cm (eccentricity ratio of 0.0 to 0.3), and the lateral reinforcement ratio between 0.0% and 0.84%, with a good or an insulated bond established for the beam reinforcement at the joint. Table 1 is a summary of the specimens. With all specimens, the beam cross-section was set to 300×750 mm, the column cross section to 800×700 mm, and the distance between contraflexural points to 4500 mm for the beams and 2730 mm for the columns. The reinforcement arrangement and material characteristics shown on Table 2 are based on experimental data, and large yield strengths were used for beam and column reinforcements to suit the objective of this research.

Analytical Methods

A 3-dimensional FEM analysis program developed by Yu and Noguchi *et al.* (Yu and Noguchi 2004, 2008) was used for the analysis code. As for material modeling, eight-node isoparametric solid elements were used to model the concrete, and an orthotropic model based on equivalent uniaxial strain was used for the constitutive law. The 5-parameter model by Willam-Warnke *et al.* (Willam and Warnke 1974) was used for the failure criteria, the Saenz equation (Saenz 1964) for the ascending section of the compression side, and the Kent-Park model (Park and Priestley 1982) for the descending section. The model proposed by Okamura-Maekawa (Okamura and Maekawa 1985) was used for post-crack tensile stiffness of concrete, and the Yamada-Aoyagi model (Yamada and Aoyagi 1983) was used for shear stiffness at the crack surface. See reference item (Noguchi 2003a, 2003b, 2008) for details of models and related literatures. The reinforcement was modeled as a 2-node truss element, and a bilinear model was used for the stress-strain relationship. The reinforcement-concrete bond characteristics were expressed by introducing bond-link elements between the nodes of elements.

Element discretization and boundary conditions are shown in Fig. 1. An antisymmetric shear force was applied in-plane at the center node of the beam cross-section at each of the two end sections of the beam. The column head and column base were pin-supported at the center node of the column cross-section. The column axial force was held constant at 10% of σ_B concrete compressive strength.

Analytical Results

Story Shear Force - Story Drift Angle Relationships

Fig. 4 shows the relationship between story shear Q_c and story drift angle R in a specimen having a good bond and a specimen having an insulated bond. Other specimens have a $Q_c - R$ curve with a similar form to that of the specimen E00, which has a good bond; therefore, Fig. 5 shows the relationship between the maximum story shear Q_{cu} (normalized from specimen hoop3, which has $p_{jw}=0.84\%$) and the lateral reinforcement ratio p_{jw} of the joint, and Fig. 6 shows the relationship between the Q_{cu} (normalized from non-eccentricity) and the eccentricity ratio. A comparison between the analytical and experimental results was examined in reference item

(Hong and Noguchi 2008), where it is shown that load-drift relationships and failure modes during repeated load mostly correlate well. In Fig. 4, the Q_{cu} for the specimen UNB having a good bond is approximately 1.1 times the joint shear strength calculated by AIJ guideline equation (AIJ 1999). In the case of an insulated bond, the ultimate strength is 17% lower than for a good bond. Of the two stiffness change points in the Q_c - R curve (points 1 and 2 in the diagram) before ultimate strength, point 1 indicates flexural cracking at the joint-end of the beam, and point 2 indicates where cracking begins to occur in virtually the entirety of the joint panel. In Fig. 5, Q_{cu} increases with increasing p_{jw} up to $p_{jw}=0.4\%$, but levels off after that and does not increase much higher. At $p_{jw}=0.0\%$, the ultimate strength has fallen by 17%. In Fig. 6, Q_{cu} falls proportionally to the eccentricity ratio, with the ultimate strength falling to 32% at eccentricity ratio of 0.31.

Stress σ_a in the Direction of the Strut in the Joint-Section Concrete

In this research, the stress component in the direction of the strut is calculated and defined as strut-direction compressive stress σ_a , to account for the fact that the direction of the principle compressive stress σ_3 vector in the joint-section concrete is not necessarily aligned with the direction of the strut throughout the panel. The direction of the strut is defined as the direction of the σ_3 vector in the concrete at the center of the joint. The distribution of σ_a in the diagonal cross-section (see Fig. 2) at ultimate strength is shown in Fig. 3.

In all joints with no eccentricity, the stress intensity increases in the vicinity of the center of the cross-section, and the stress intensity decreases at the center due to concrete crushing. The specimen E00 that has a good bond and the specimen hoop3 that has a large amount of lateral reinforcements transmit stress virtually throughout the cross-section; however, the specimen UNB that has an insulated bond has regions in both ends in the depth direction of the diagonal cross-section that do not transmit stress, and the specimen hoop0 that has no lateral reinforcement has regions in both ends in the width direction of the diagonal cross-section that do not transmit stress.

In the specimen E15, which has eccentricity, the stress intensity in the eccentric side is higher than in the joint where there is no eccentricity, and a fall in stress intensity due to concrete crushing is observed in the side surface of the beam. In addition, in the non-eccentric side, no stress transmission is observed in a region occupying about 30% of the width of the cross section. Therefore, it is thought that in the eccentric side of the eccentric joint, concrete crushing is hastened because of the tendency for the stress to be transmitted through the eccentric side and because of an accumulation in torsional stress due to torsional moment, and that the cross-sectional area that effectively transmits stress decreases, thereby decreasing the ultimate strength.

Examination of Strut-Direction Stress σ_a within Regions

With regards to the distribution of σ_a in the diagonal cross-section at ultimate strength shown in Fig. 3, regions within which σ_a exceeds various reference stress intensities of between $0.12F_c$ and $0.4F_c$ are examined in terms of the cross-sectional area of each region and the resultant force of σ_a in each region. (F_c : concrete compressive strength) Fig. 7 shows the area of

the region for each reference stress and Fig. 8 shows the resultant force of σ_a in each region. The bar graphs show the story shear strength. In Figs. 1 and 2, both the area of the region and the compressive force transmitted within the region exhibit variation between each specimen at a reference stress of $0.12F_c$; the variations are similar to that in story shear strength. The variation between specimens, in the area of the region and the compressive force transmitted within the region, tend to diminish with increasing reference stress.

At a reference stress of $0.4F_c$, the areas of the regions are almost consistent at just under 20% of the total diagonal cross-sectional area across all specimens, and the compressive force transmitted within the regions are also almost consistent, at just under 40% of the total cross-sectional resultant force for the specimen E00. With all specimens, distribution of σ_a within the regions is almost uniform, and the average stress intensity is about $0.5F_c$. Accordingly, it is thought that within the joint, there exists a region with a cross-sectional area that does not depend on specimen parameters, and in which the amount of compressive force transmitted within that cross-section remains almost consistent. In this research, this region is defined as the intrinsic strength region.

Examination of σ_a in Region with Reference Stress $0.12F_c$

Here, an equivalent rectangular cross-section with an equal area is examined as a substitute for the region, as both the area of the region with reference stress $0.12F_c$ and the compressive force transmitted therein show good correlation with the story shear strength. The equivalent rectangular cross-sections for each of the joints are shown in Fig. 3, and the depths (lengths in the depth direction of the strut) and widths (lengths in the width direction of the strut) of the cross-sections are shown in Figs. 9 and 10.

While the depths of rectangular cross-sections shown in Fig. 9 range between 0.74 and 0.84 for joints with good bond, the figure for the specimen UNB, which has an insulated bond, is extremely small, at 0.5. The widths of equivalent rectangular cross-sections, shown in Fig. 10, range between 0.75 and 0.79 for specimens with p_{jw} of 0.3% or above and with no eccentricity. In contrast, for specimens with eccentric joints, the width decreases with increasing eccentricity; and for the specimen hoop0 for which $p_{jw}=0.0\%$, the width is extremely small, at 0.6.

These observations indicate that bond characteristics mainly have an effect in the strut-depth direction, and that the depth decreases as bond deterioration progresses. They also indicate that the amount of lateral reinforcement and the eccentricity mainly have an effect in the strut-width direction, and that the width decreases with decreasing lateral reinforcement and with increasing eccentricity.

Derivation of a Beam-Column Joint Shear Strength Equation

A shear strength equation V_{ju} for an RC beam-column joint is derived, based on the results of the above investigations. V_{ju} is expressed as the following equation:

$$V_{ju} = F_j \times S_j \times \beta_{jt} \quad (1)$$

Here, F_j represents the reference shear stress intensity for the shear strength, S_j represents the effective cross-section area (product of the effective depth D_j of the joint and the effective width b_j of the joint), and β_{jt} represents the ratio of decrease in ultimate strength due to torsional stress.

Effective Depth D_j of the Joint

D_j is assumed to be a function of an indicator representing the degree of bond deterioration. Taking 0.8D (D is the column depth), which is the equivalent rectangular cross-section depth for the specimen E00 with a good bond, as its upper limit, and 17%, which is the ratio by which the ultimate strength of the specimen UNB with an insulated bond is lower than that of the specimen E00, as its lower limit, and interpolating between the two, D_j is represented by the following equation.

$$D_j = 0.66D + 0.14D \times S \quad (2)$$

Here, S is set to a value between 0.0 and 1.0 as an indicator representing the degree of bond deterioration.

Effective Width b_j of the Joint

b_j is represented by the following equation (see Figs. 11 and 12).

$$b_j = b_b + b_{a1} + b_{a2} \quad (3)$$

Here, if $\tan\beta \leq 2b_{si}/D_s$, Eq.4 applies.

$$b_{ai} = \tan\beta \cdot D_s/4 \quad (4)$$

If $\tan\beta > 2b_{si}/D_s$, Eq. 5 applies.

$$b_{ai} = (1 - b_{si}/D_s \cdot \cot\beta) \cdot b_{si} \quad (5)$$

The angle β , within which stress is effectively transmitted from the side surface of the beam, is represented as follows.

$$\beta = 0.15\pi + 18.5\pi \cdot p_{jw} \quad (6)$$

Here: b_b , D_s : Column width, diagonal cross-section depth
 b_{si} : Length from side surface of beam to the parallel side surface of column
 b_{ai} : Length from side surface of beam, representing the range of angle β within which stress is effectively transmitted from the side surface of the beam, substituted by a rectangular cross-section having an equal area.
 p_{jw} : Lateral reinforcement ratio at the joint; a value of 0.003 is used if $p_{jw} > 0.003$.

Eq. 6 for the angle β was set up using the ultimate stress strength of the specimen E00

with $p_{jw}=0.3\%$ and that of the specimen hoop0 with $p_{jw}=0.0\%$ as upper and lower limits.

Ratio of Decrease of Ultimate Strength due to Torsional Stress

The decrease in ultimate strength in eccentric joints is assumed to be caused by: the term 1. torsional stress resulting from torsional moment, cumulating on top of shear stress resulting from shear force, and the term 2. decrease in cross-sectional area that effectively transmits stress because of a tendency for stress to be transmitted to the eccentric side. The effect of the above term 2 has already been taken into account in the proposed Eq. 3 to 5 for b_j . Here, the decrease in ultimate strength due to the term 1 is defined as the ultimate strength decrease rate β_{jt} due to torsional stress. β_{jt} is represented by the following equation as a ratio of areas below curves f_e and f_0 shown in Fig. 13.

$$\beta_{jt} = \frac{\int f_e}{\int f_0} = \frac{\int f_{e0}}{\int f_0} \quad (7)$$

Here, f_e : Distribution curve of stress σ_a at ultimate shear strength, of an eccentric joint subject to torsional moment

f_{e0} : Distribution curve of stress σ_a when the shear stress component resulting from torsional moment is removed from f_e

f_0 : Distribution curve of stress σ_a at ultimate shear strength, of an eccentric joint, if it is assumed that no torsional moment acts on it

Because calculation of $\int f_{e0}$ and $\int f_0$ in Eq. 7 is difficult, the following equation is used as an approximation.

$$\beta_{jt} = \frac{\int f_{e0}}{\int f_0} \approx \frac{\sigma_{e0}}{\sigma_{\max}} \quad (8)$$

$$\sigma_{e0} = \sigma_{\max} - \tau_{jt} \quad (9)$$

Here, σ_{\max} : Maximum stress intensity at ultimate shear strength. The average stress intensity of σ_a in the intrinsic strength region is used. Assumed to be $0.5F_c$ from the section 6.

τ_{jt} : Average stress intensity within the intrinsic strength region resulting from torsional moment

The average stress intensity τ_{jt} within the intrinsic strength region resulting from torsional moment is obtained from the average value of torsional stress within the intrinsic strength region after determining the size of the region. The size of the intrinsic strength region is assumed to be determined by the beam and column widths. Torsional stress in the rectangular cross-section can be obtained from the torsional moment using an approximation by substituting with an ellipse having an equal area. The torsional moment resulting from joint eccentricity is obtained as a product of joint shear and eccentricity (AIJ 1998).

Reference Shear Stress Intensity F_j for the Joint Shear Strength

From the analytical results obtained by FEM for the specimen E00 using compressive

strength σ_b as a parameter and experimental data for non-eccentric RC plane column-beam joints obtained from previously published papers, the relationship between F_j and σ_b is obtained based on the proposed b_j and shown in Fig.14. In the case of the experimental data, F_j is more dispersed at higher concrete strength σ_b . Based on the analytical data, an estimate equation for F_j is obtained using regression analysis, and shown in Eq. 10. Because the analytical results are based on the constitutive law for normal-strength concrete, Eq. 10 applies to instances where $\sigma_b \leq 60\text{N/mm}^2$.

$$F_j = 1.69 \times \sigma_b^{0.538} \quad (10)$$

Conclusions

Three-dimensional FEM analysis was conducted on joint shear failure type plane RC plane beam-column joints. In addition to examining crushing of joint-section concrete at ultimate shear strength and its effective compression strength, the stress component in the direction of the strut was analyzed quantitatively, and the effects of joint-section bond characteristics of the beam reinforcement and the amount of lateral reinforcement on stress distribution at ultimate strength were examined. The analytical results were used to propose an estimation equation for joint shear strength.

References

- AIJ(Architectural Institute of Japan), 1998. Recommendation to RC Structural Design after Hanshin-Awaji Earthquake Disaster -Cause of particularly noticed damages and corresponding RC structural design details-, 602pps.
- AIJ(Architectural Institute of Japan), 1999. Design Guidelines for Earthquake Resistant Reinforced Concrete Buildings Based on Inelastic Displacement Concept, 440pps.
- Darwin, D., and D. A. W. Pecknold, 1974. Inelastic Model for Cyclic Biaxial Loading of Reinforced Concrete, *A Report on A Research Project Sponsored by the NSF*, University of Illinois.
- Hong, Jie, T. Kashiwazaki, and H. Noguchi, 2006. Three-dimensional FEM Analysis of Seismic Performance of RC Eccentric Beam-column Joints under Cyclic loading, *Proceedings of the Japan Concrete Institute*, 28, 319-324.
- Hong, J., T. Kashiwazaki, and H. Noguchi, 2007. Study on Seismic Performance of RC Beam-Column Joints with Eccentric Beams Using 3-D FEM Analysis, *Proceedings of AIJ Annual Convention*, 605-608.
- Hong, Jie, T. Kashiwazaki, and H. Noguchi, 2008. Analytical Study on of Seismic Performance of RC Eccentric Beam-column Joints with Lateral Beams under Cyclic loading, *Proceedings of the Japan Concrete Institute*, 30, 331-336.
- Ihzuka, T., and H. Noguchi, 1992. Nonlinear Finite Element Analysis of RC Members with Normal to High Strength Materials, *Proceedings of the Japan Concrete Institute*, 14(2), 9-14.
- Ishida, K., K. Shima, K. Higashi, and S. Fujii, 2001. Full Size Test on RC Interior Beam-column Joints, *Proceedings of the Japan Concrete Institute*, 23 (3), 343-348.
- Morita, S., and T. Kaku, 1975. Bond-Slip Relationship Under Repeated Loading, *Transactions of the Architectural Institute of Japan*, 299, 15-24.
- Noguchi, H., 2003a. Three-Dimensional FEM Analysis of RC Beam-Column Joints Subjected to Two-Directional Loads, *Finite Element Analysis of Reinforced Concrete Workshop*, SP-237, American Concrete Institute, Farmington Hills, MI, 149-164. (CD-ROM)

- Noguchi, H., 2003b. Toward a High-Quality FEM Analysis of RC Members Subjected to Reversed Cyclic Shear, *Proceedings of EURO-C 2003, Computational Modelling of Concrete Structures*, Bicanic et al. (eds.), 901-908.
- Noguchi, H., T. Kashiwazaki, and J. Hong, 2008. FEM Analysis of Three-Dimensional Interaction of RC Frames Subjected to Multi-Directional Cyclic Loading, *Proceedings of the Fourteenth World Conference on Earthquake Engineering*, Beijing, China, Paper 14-0064, 8 pps. (CD-ROM)
- Okamura, H., and K. Maekawa, 1985. Nonlinear Finite Element Analysis of Reinforced Concrete Structures, *Proceedings of Japan Society of Civil Engineering*, 360(3), 1-10.
- Park, R., M. J. N. Priestley, and W. D. Gill, 1982. Ductility of Square-Confined Concrete Columns, *Journal of the Structural Division, Proceeding of ASCE*, ST4, 930-950.
- Saenz, L. P., 1964. Discussion of 'Equation for the Stress-Strain Curve of Concrete, by P. Desayi and S. Krishnan, *ACI JOURNAL, Proceedings*, 9, 1229-1235.
- Sato, T., and N. Shirai, 1978, Elasto-Plastic Behavior of RC Shear Walls, *Summaries of Technical Papers of Annual Meeting*, C-2, Architectural Institute of Japan, 1615-1618.
- Uchida, K., and H. Noguchi, 1998. Analysis of a Two Story, Two Bay Frame Consisting of Reinforced Concrete Columns and Steel Beams with Through-Beam Type Beam-Column Joints, *Journal of Structural and Construction Engineering*, Architectural Institute of Japan, 514, 207-214.
- Willam, K. J., and E. P. Warnke, 1974. Constitutive Model for the Triaxial Behaviour of Concrete, *Proceedings of IABSE Seminar on 'Concrete Structures subjected to Triaxial Stresses'*, Bergamo, Italy, 19, 1-31.
- Yamada, K., and Y. Aoyagi, 1983. Shear Transfer across Cracks, *Proceedings of Japan Concrete Institute Second Colloquium on Shear Analysis of RC Structures*, 19-28.
- Yu, Y., T. Kashiwazaki, and H. Noguchi, 2004. Development of FEM Analytical Program on RC Structural Elements Subjected to 3 Dimensional Cyclic Loads (Part 1, 2), *Summaries of Technical Papers of Annual Meeting*, C-2, 67-70.

Table 1. Properties of specimens.

Test specimens	Eccentric distance (eccentricity ratio)	Pw (%)	Property of bond
E00	0 cm (0.0)	0.3	Normal
E05	5 cm (0.06)	0.3	Normal
E10	10 cm (0.13)		
E15	15 cm (0.19)		
E20	20 cm (0.25)		
E25	25 cm (0.31)		
UNB	-	0.3	Insulated
hoop0	-	0	Normal
-	-	0.05~0.4	
hoop3	-	0.84	

Table 2. Materials of concrete and reinforcement.

Test specimens	Column (800×700 mm)		Beam (300×750 mm)		Pw (%)
	Main reinforcement	Hoop	Main reinforcement	Stirrup	
Reinforcement (Yield strength)	14-D29 (high)	2-D13 at 100 (365N/mm ²)	8-D25 (high)	2-D13 at 100 (365N/mm ²)	0~0.84 (365N/mm ²)
Concrete	Compressive stress (N/mm ²)	Strain at Compressive stress (μ)	Young's modulus (N/mm ²)	Tensile stress (N/mm ²)	
	33.4	2,000	25,900	2.21	

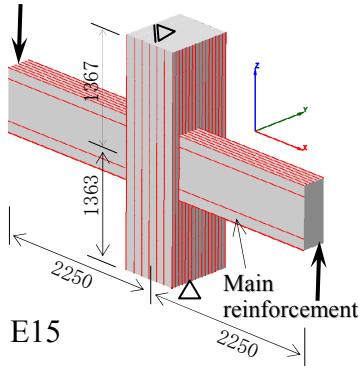


Figure 1. Finite element idealization and boundary condition.

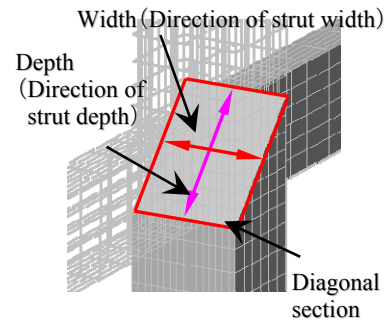


Figure 2. Diagonal section.

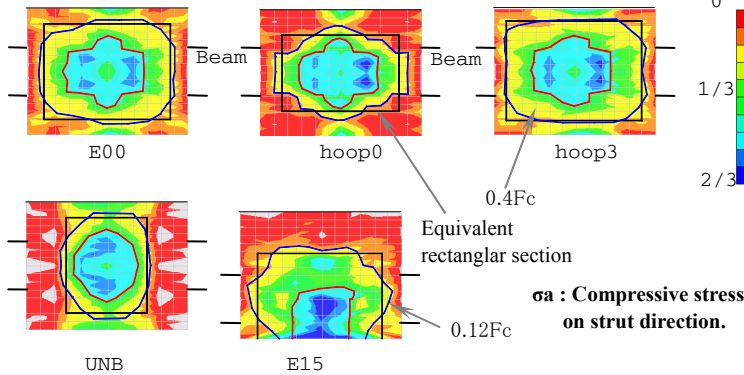


Figure 3. Distribution of σ_a on diagonal section (at Q_{cu}).

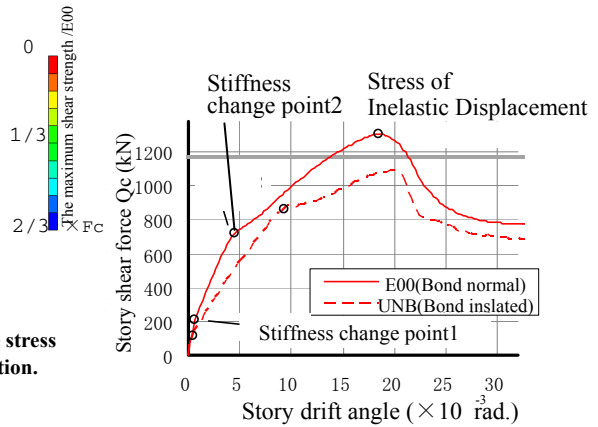


Figure 4. Relationships between story shear force and story drift angle.

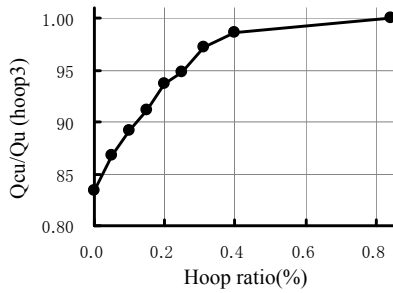


Figure 5. Relationships between story shear force of hoop3 and raio of hoop.

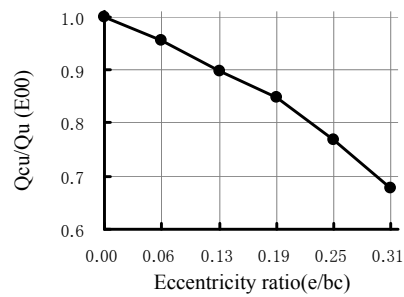


Figure 6. Relationships between story shear force of E00 and ratio of eccentricity.

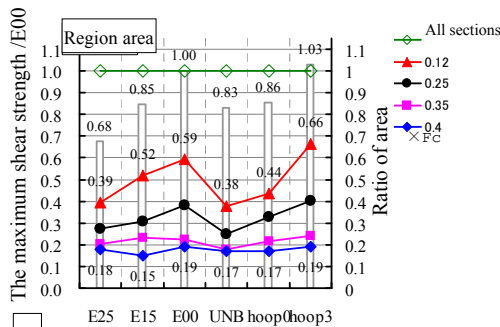


Figure 7. Region area.

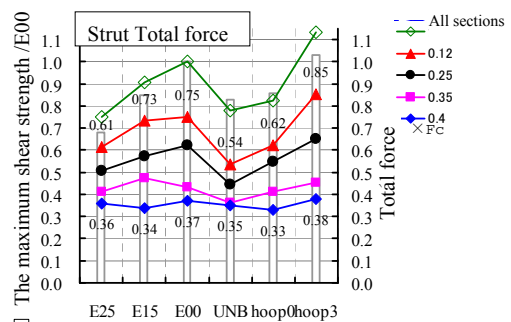


Figure 8. Resultant force σ_a in each region.

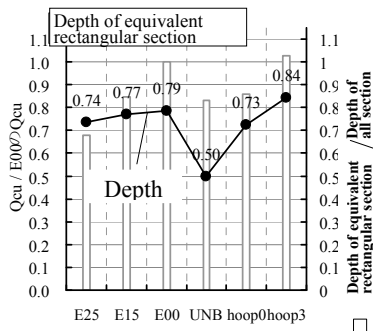


Figure 9. Depth of equivalent rectangular section.

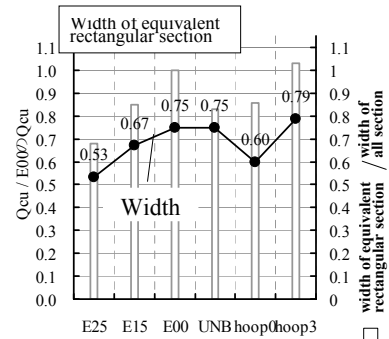


Figure 10. Width of equivalent rectangular section.

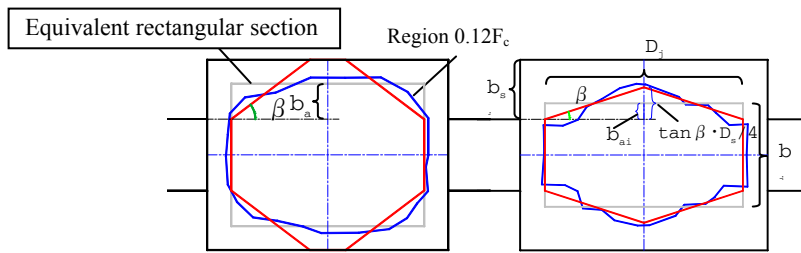


Figure 11. Specimen E00. ($p_w=0.3\%$)

Figure 12. Specimen hoop0. ($p_w=0.0\%$)

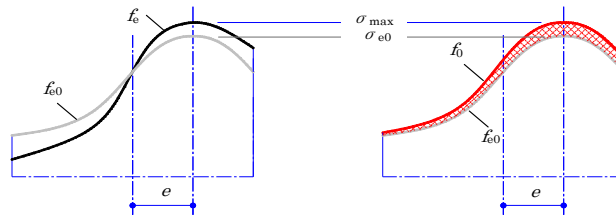


Figure 13. Distribution of stress σ_a at the maximum joint shear strength.

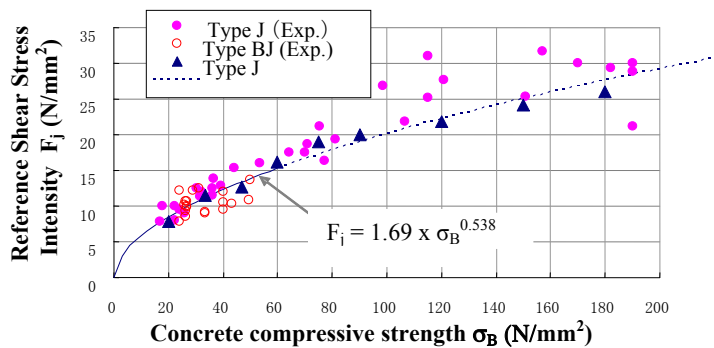


Figure 14. Relation F_j - σ_B for interior beam-column joints.